

Measurement of the mechanical properties of isolated tectorial membrane using atomic force microscopy

Rachel Gueta*, David Barlam†, Roni Z. Shneck‡, and Itay Rouso*§

*Department of Structural Biology, Weizmann Institute of Science, Rehovot 76100, Israel; and Departments of †Mechanical Engineering and ‡Materials Engineering, Ben-Gurion University of the Negev, Beer-Sheva 84105, Israel

Edited by A. J. Hudspeth, The Rockefeller University, New York, NY, and approved August 10, 2006 (received for review April 30, 2006)

The tectorial membrane (TM) is an extracellular matrix situated over the sensory cells of the cochlea. Its strategic location, together with the results of recent TM-specific mutation studies, suggests that it has an important role in the mechanism by which the cochlea transduces mechanical energy into neural excitation. A detailed characterization of TM mechanical properties is fundamental to understanding its role in cochlear mechanics. In this work, the mechanical properties of the TM are characterized in the radial and longitudinal directions using nano- and microindentation experiments conducted by using atomic force spectroscopy. We find that the stiffness in the main body region and in the spiral limbus attachment zone does not change significantly along the length of the cochlea. The main body of the TM is the softest region, whereas the spiral limbus attachment zone is stiffer, with the two areas having averaged Young's modulus values of 37 ± 3 and 135 ± 14 kPa, respectively. By contrast, we find that the stiffness of the TM in the region above the outer hair cells (OHCs) increases by one order of magnitude in the longitudinal direction, from 24 ± 4 kPa in the apical region to 210 ± 15 kPa at the basilar end of the TM. Scanning electron microscopy analysis shows differences in the collagen fiber arrangements in the OHC zone of the TM that correspond to the observed variations in mechanical properties. The longitudinal increase in TM stiffness is similar to that found for the OHC stereocilia, which supports the existence of mechanical coupling between these two structures.

cochlea | collagen fibers | indentation | hearing

The tectorial membrane (TM) is a heterogeneous and gelatinous extracellular matrix. It is located in the cochlea, which transduces mechanical audio stimuli into an electrical signal. Under physiological conditions, 97% of the weight of the TM is water, whereas the remainder is composed of proteins and proteoglycans (1). Nearly half of these proteins are collagens, principally of type II, which form fibrils that are assembled along the radial direction (Fig. 1A); at the surface of the TM, which faces away from the hair-cells, they form a mesh-like structure called the covering net.

Structurally, the TM spans the entire length of the cochlea and is $\approx 100 \mu\text{m}$ wide and $50 \mu\text{m}$ thick. It is strategically situated over the sensory cells of the cochlea: the outer (OHCs) and inner (IHCs) hair cells (Fig. 1B). The electromotility of OHCs is thought to play a central role in the cochlear mechanical-electrical transduction process (2, 3), whereas IHCs synapse directly with the auditory nerve (4). Upon auditory stimulation, deflection of the stereocilium bundles, which exist both in OHCs and IHCs, directly converts the mechanical energy into an electrical signal. This conversion is the physiological function of these cells. An additional function of the OHCs is electromechanical transduction. Whereas the stereocilia of OHCs are physically embedded in the lower surface of the TM, the stereocilia of the IHC are, at most, lightly attached. It is thought that OHC stereocilia are deflected by direct displacement of the TM, whereas IHC stereocilia are deflected by the flow of the

fluid in the subtectorial space. Considering the above, the TM is likely to play an important role in delivering sound-induced mechanical stimuli to OHC hair bundles, as well as in communicating between OHC and IHC hair bundles. Further support for the important role of the TM in hearing is obtained from recent studies, which have shown that mutations in proteins of the TM cause auditory impairments (5–8).

In many models of cochlear micromechanics, the mechanical properties of the TM are theoretically modeled. These models can be grouped into three main categories based on their description of the role of the TM: (i) The TM as a rigid and stiff body which rotates during sound stimulation around the spiral limbus attachment region. This rotation generates a shearing force against the OHC stereocilium bundles (9–13). (ii) The TM as a resonant mass: in these models, the TM is merely a stationary mass load. Vertical movements of OHCs induce bending of the stereocilia with respect to the TM (14–17). In the third group (iii), the TM is considered to be an isolated mass on top of the hair bundles. In these models, the TM is completely flexible and therefore mechanically unimportant (18).

Attaining comprehensive knowledge of the mechanical properties of the TM is central to understanding its interactions with neighboring structures, such as OHC stereocilia, and thus its role in cochlear micromechanics. The mechanical properties of the TM have previously been studied by using mechanical probes, including hairs and needles (19), and glass pipettes (20). One of the major shortcomings of these studies is the nonphysiological large-scale displacements (tens of microns) that were used to characterize TM properties. Recently, Freeman *et al.* (21) measured the stiffness of isolated mouse TM samples, during sub-micrometer displacements, using magnetic beads having a diameter of $10 \mu\text{m}$. More recently, the shear modulus of TM samples isolated from guinea pigs was probed with an atomic force microscope (AFM) using nano- and microscaled indenters ($\approx 20 \text{ nm}$ and $\approx 10 \mu\text{m}$ in diameter, respectively) (22). In that AFM study, the mechanical properties of the TM appeared similar as a function of longitudinal position. In light of their finding, it is not clear how different regions in the TM can have similar mechanical properties and at the same time interact, in a nondestructive manner, with hair bundles that oscillate at $\approx 20 \text{ Hz}$ in one region and $\approx 20 \text{ kHz}$ in another.

In this study, the stiffness and Young's modulus of TM samples isolated from mice were analyzed through indentation-type experiments conducted with an AFM tip. We show that, in the

Author contributions: I.R. designed research; R.G. performed research; R.G., D.B., R.Z.S., and I.R. analyzed data; and R.G., D.B., R.Z.S., and I.R. wrote the paper.

The authors declare no conflict of interest.

This paper was submitted directly (Track II) to the PNAS office.

Abbreviations: TM, tectorial membrane; OHC, outer hair cell; IHC, inner hair cell; AFM, atomic force microscope.

§To whom correspondence should be addressed. E-mail: itay.rouso@weizmann.ac.il.

© 2006 by The National Academy of Sciences of the USA

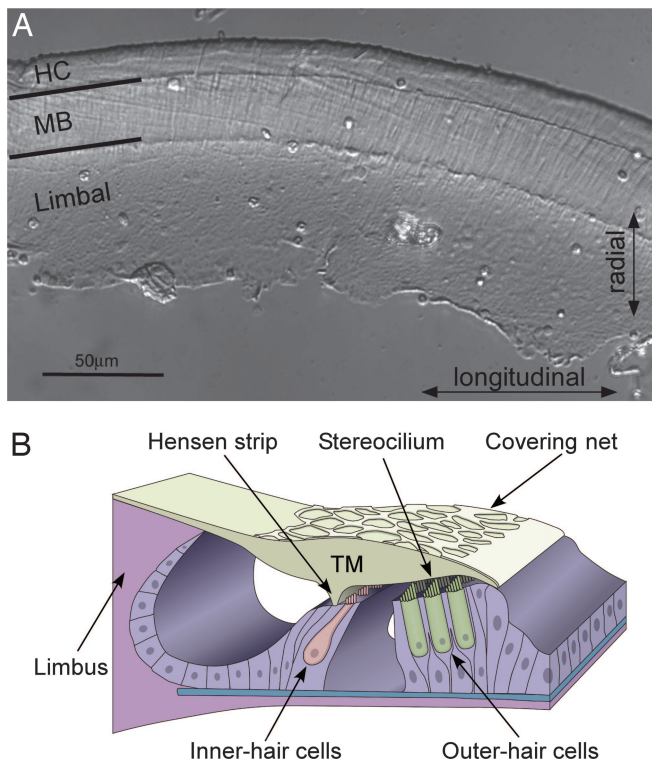


Fig. 1. Photomicrograph of the TM and schematic representation of the organ of Corti. (A) A phase contrast transmitted light microscope image of a TM segment isolated from the basal region of the cochlea. Measurements were grouped together according to their radial zone: the outer hair cells zone (labeled HC), the tectorial membrane main body (labeled MB), and the spiral limbus attachment area (labeled limbal). The longitudinal and radial directions of the TM are correspondingly shown with double-headed arrows. (B) Schematic representation of the organ of Corti, showing the location of the TM with respect to the outer- and inner-hair cells.

radial direction, the limbal zone has the highest stiffness, whereas the main body of the TM has the lowest stiffness. More importantly, we find that in the longitudinal direction, the elasticity of the TM in the OHC zone is ≈ 10 times as large in the basal region as in the apical region. Scanning electron microscopy (SEM) analysis reveals substantial differences in the arrangement of collagen fibers along the structure, which correlated to the observed variations in mechanical properties.

Results and Discussion

The Stiffness of the TM. To measure the mechanical properties of the TM, an AFM probe was positioned above the TM surface and force–distance curves were acquired. A typical averaged force–distance curve for a TM indented by a nanoscale-sized probe is shown in Fig. 2, together with the corresponding cantilever deflection curve (see *Supporting Text* and Fig. 5, which are published as supporting information on the PNAS web site, for more details). The main advantage of measuring mechanical properties with an AFM is its ability to apply low forces and penetration depths as well as the possibility of using indenters of various sizes. A nanometer-scaled silicon nitride tip with a radius of ≈ 20 nm is approximately the same magnitude as an individual collagen fiber (≈ 50 nm diameter), and thus can probe the properties of structures at the level of a few collagen fibers. The averaged point stiffness of the TM measured with a nanometer-scaled tip is shown in Fig. 3A. Within each longitudinal zone, the differences between the stiffness values obtained in the radial direction are minute. However, even at the level of few collagen fibers, a small gradient in the stiffness of the TM is detectable

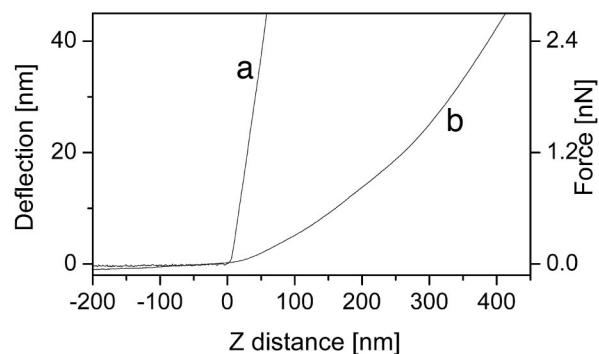


Fig. 2. Measuring the stiffness of the tectorial membrane (TM) by indentation type experiments. Typical averaged force distance curves for deflection of the cantilever (curve a) and for a TM sample measured in the MB zone (curve b). The curves were shifted along the z axis to set the tip-sample contact point (Z_0) to a distance of zero. In the case of force–distance curves for the TM, Z_0 was derived from fitting the data with an appropriate model. For each experiment, ≈ 150 curves were acquired. The TM indentation depth is defined as the difference between the z position of the TM and cantilever deflection at a given loading force.

in the longitudinal direction. The TM at the apical region is slightly softer than at the basal region. The differences in stiffness values between the apical and mid-turn, and mid-turn

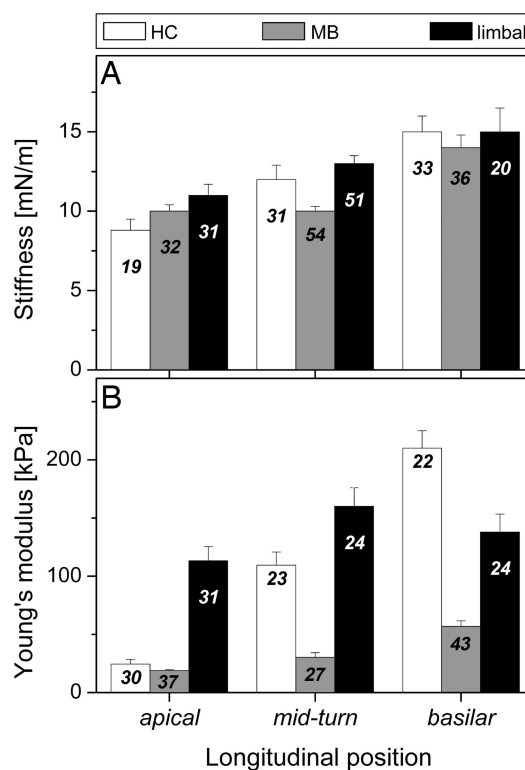


Fig. 3. The longitudinal and radial distributions of TM mechanical properties. (A) The averaged point stiffness values of the TM measured with a nanometer scaled probe (radius of 20 nm). (B) Young's modulus values of the TM measured with a micrometer scaled probe (radius of 1 μ m). Results are grouped into apical, mid-turn, and basal regions according to their longitudinal position. Each longitudinal group is further divided into the following radial zones: HC (white), MB (gray), and limbal (black). The bars represent the standard error, and the number of samples analyzed is indicated by the number shown in each column. See Fig. 6, which is published as supporting information on the PNAS web site, for more details.

and basilar are significant only at confidence levels below 98% ($P = 0.015$) and 93% ($P = 0.064$), respectively.

We next studied the stiffness of the TM as sensed by the stereocilium bundle of a single OHC. To measure cumulative properties from such an area, a larger indenter, capable of deforming an area similar to that deformed by a single bundle, was used. To estimate the area deformed by a given indenter, we simulated our indentation experiments using finite element analysis. The TM was modeled as an elastic material having a Young's modulus value which was experimentally derived from the point stiffness measured by using the nanometer-scaled probe. A cross-section of the deformed model of the TM shows that an area with a radius of $\approx 3 \mu\text{m}$ is affected by the $2\text{-}\mu\text{m}$ spherical bead. The simulated deformed area is similar to the imprint area of a single stereocilium bundle (Fig. 7, which is published as supporting information on the PNAS web site). A clear correlation between the stiffness of the TM and its longitudinal and radial position is observed when a $2\text{-}\mu\text{m}$ probe is used (Fig. 3B). Specifically, we find that in the radial direction, the main body of the TM is the softest region regardless of longitudinal position. In contrast, the limbal zone of the TM has the largest Young's modulus along its entire length, except in the basal region, where the HC zone is the stiffest. Interestingly, the stiffness of the TM at the HC zone gradually increases in the longitudinal direction. The Young's modulus of the HC zone at the apical end of the TM ($24 \pm 4 \text{ kPa}$) is only about one-tenth of that of the modulus of this zone at the basal end ($210 \pm 15 \text{ kPa}$). Student *t* test showed that the differences in stiffness values along the longitudinal direction are significant ($P < 0.0001$ at 99.9% confidence level). Overall, the stiffness of the TM is $\approx 1\text{--}10\%$ that of cartilage (23), despite their similar biochemical and structural compositions. The increased stiffness of cartilage compared with TM is probably because of the lower water content of the former (80% compared with 97%). Additionally, a transversal orientation of collagen fibers in cartilage may increase its stiffness.

Recently, the shear moduli of TM samples isolated from guinea pigs were estimated from similar indentation experiments conducted with an AFM (22). Our nanoindentation results agree well with their results (for the purposes of comparison between the two studies, we have analyzed our data using their shear modulus model). However, there is no agreement between the microindentation results presented in this work and theirs. Particularly, they did not observe any correlation in the HC zone between the stiffness of the TM and its longitudinal location. We propose that the discrepancy between the two sets of microindentation results is probably a result of the different indenter sizes used in these two studies. Our microindentation measurements were carried out by using a $2\text{-}\mu\text{m}$ probe, whereas Shoelson *et al.* (22) used a $10\text{-}\mu\text{m}$ probe. Finite-element analysis suggests that the area deformed by a $2\text{-}\mu\text{m}$ probe during indentation of $\approx 350 \text{ nm}$ has a diameter of $\approx 6 \mu\text{m}$. In contrast, our finite-element analysis suggests that indentation by a $10\text{-}\mu\text{m}$ probe to an equal depth will deform a significantly larger area, having a diameter of $\approx 20 \mu\text{m}$. Such a large area is comparable to the entire width of the TM. Therefore, measurements carried out with $10\text{-}\mu\text{m}$ beads probably include contributions from other radial zones, and thus represent an averaged radial stiffness. Under such conditions, it is possible that the contribution of what we find to be a consistently soft MB zone may mask the gradual increase in the stiffness of the TM in the HC zone.

The Ultrastructure of the TM. To assess whether there is a correlation between the mechanical properties of the TM and its ultrastructure, TM samples isolated from the apical and basal regions were studied by using SEM. Samples isolated from the apical region of the cochlea with the covering net facing up (toward the AFM probe) and down (toward the glass slide) are

shown in Fig. 4A and B, respectively, whereas Fig. 4C and D shows TM samples isolated from the basal region with the covering net facing up and down, respectively. Radial zones were determined according to the same criteria as used for our AFM studies. Analysis of the fiber arrangements in the limbal (lim) and MB zones shows no significant changes with longitudinal zone (apical or basal), but indicates substantial differences between these two radial zones. We find that the collagen fibers in the limbal zone are arranged in a tightly packed manner, whereas in the main body of the TM (MB) they form parallel striations. Fig. 4B and D show this parallel arrangement in the MB zone as seen on the stereocilium imprint side, and a similar structure can be observed below the covering net (the thin mesh-like layer of fibers) in the insert to Fig. 4C. The elongated features (arrow) along the longitudinal direction of the TM seen in Fig. 4B and D, between the stereocilium imprint region (HC) and the main body (MB), is the Hensen stripe.

Interestingly, the most dramatic structural changes along the length of the TM are seen in the HC zone. Analysis of the covering net side shows that, in the apical region (Fig. 4A), the HC zone fibers are arranged in a mesh-like structure similar to their arrangement in the upper layer of the MB zone (Fig. 4C *Inset*). Moving toward the basal region, the transverse fibers gradually become closer to each other until they merge into an apparently uniform homogenous matrix (Fig. 4C; HC zone). This area is defined as the marginal band. On the stereocilium imprint side of the TM, in the apical region (Fig. 4B), the fiber arrangement in the HC zone is almost indistinguishable from that in the MB zone, with thick fibers arranged in a parallel manner. In contrast, in the basal region, there are clear structural differences between the HC and the MB zones as viewed from the stereocilium imprint side. As seen in Fig. 4D, the collagen fibers in the HC zone are arranged in a tightly packed manner, whereas a parallel fiber arrangement is observed in the MB zone.

Correlation Between TM Mechanical Properties and Structure. The biochemical composition of the TM is similar throughout, in both the longitudinal and radial directions (24). Therefore, it is expected that, at resolution scales comparable to a single building block, the structure of the TM will appear very similar in all regions. As the resolution decreases, distinct "suprastructural" features become apparent due to the different packing arrangements of these building blocks. This implies that, to correlate mechanical properties and structure, the area probed in the mechanical analysis must be comparable to the scale of the distinctive structural features. It has been shown that the strength of highly hydrated proteoglycan matrices such as the TM is most significantly impacted by type II collagen fibers (24, 25). Therefore, their arrangements are probably the most relevant structural feature that should be analyzed in assessing possible correlation with mechanical properties. The deformed area during our indentation experiments is considered as the probed area in the mechanical analysis. This area was determined by using finite-element analysis, which was carried out by using the experimental mechanical properties of the TM, the tip geometry and applied indentation depths.

High-resolution SEM analysis indicates that, at the scale of several collagen fiber clusters, there are only minor structural differences along the length of the TM. We find that, when the stiffness of the TM was measured by using a nanometer-scaled probe that detects the properties from an area composed of a single cluster composed of few collagen fibers, minor changes were found along its radial and longitudinal directions (Fig. 3A). In contrast, micrometer scale analysis of TM structure shows clear morphological changes in the fiber arrangements in the radial and longitudinal directions (Fig. 4). Comparison between these structural differences and the microindentation results (Fig. 3B) indicates a correlation between TM structure, specif-

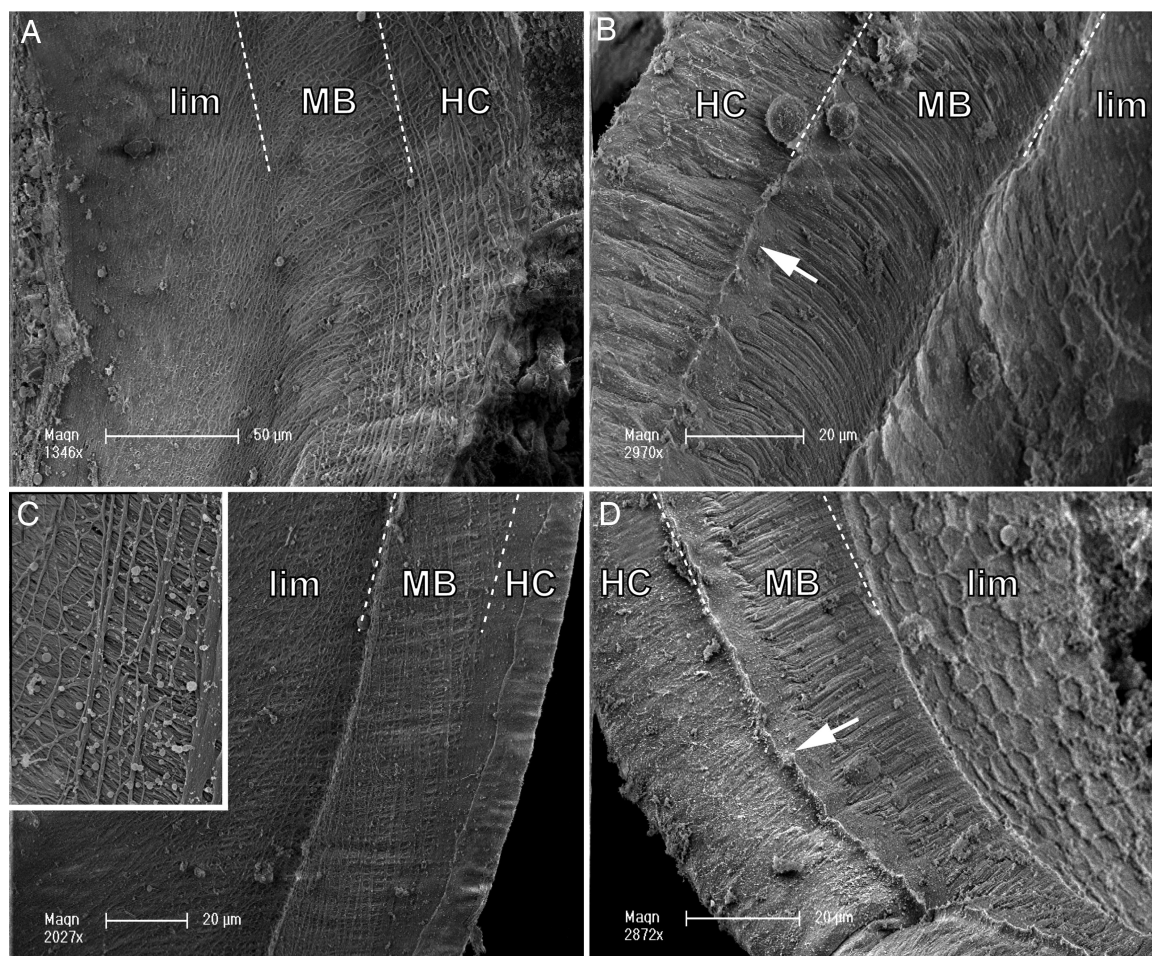


Fig. 4. Scanning electron microscopy analysis of the ultrastructure of the TM. The three radial regions, HC, MB, and limbal (lim), according to which the mechanical measurements were grouped together, are bounded by white dashed lines. (A) A segment of a TM isolated from the apical region of the cochlea, with the covering-net side facing up (toward the AFM probe). Note the similar parallel fiber arrangements in the HC zone (beneath the mesh-like upper layer) and MB zones, compared with the tightly packed arrangement visible in the limbal zone. (B) The stereocilium imprint surface (i.e., the side opposite the covering net) of a TM sample isolated from the apical region. Note the similar parallel arrangement of thick fibers in the HC and MB zones. (C) TM sample isolated from the basal region with the covering net facing up. A striking structural difference between the homogenous matrix (marginal band) seen in the HC zone and the mesh-like surface layer of the MB zone is clearly visible. (Inset) The mesh-like surface structure of the MB zone beneath which thick fibers lying in a parallel arrangement can be discerned. (D) A TM sample isolated from the basal region of the cochlea with the stereocilium imprints facing up. Similar to C, a clear difference is seen between the tight packing of the fibers in the HC zone and the parallel thick fiber arrangement observed in the MB zone beneath the covering net.

ically the collagen fiber arrangement, and mechanical properties. We find that, in the TM main body (MB zone), i.e., in the softest regions of the TM (Fig. 3B), the collagen fibers are arranged in a unidirectional parallel manner (Fig. 4). This parallel structure is maintained throughout the entire longitudinal length of the TM, together with low stiffness values. The fibers in the limbal zone are packed more tightly than in the MB zone, and are arranged in a multidirectional manner. Similarly to the MB zone, the structure of the fibers is maintained along the length of the TM. Correspondingly, the stiffness of the TM in the limbal zone does not dramatically change as a function of longitudinal position, and is higher than the stiffness measured in the MB zone (Fig. 3B). Analysis of the composition of the TM shows that collagen type II fibers exist in high amounts both in the limbal and MB zones (26). This observation supports the suggestion that differences in fiber packing, rather than in the elasticity of the fibers themselves, give rise to the different mechanical properties observed.

The most dramatic structural and mechanical differences along the length of the TM are found in the HC zone. In the

apical region (Fig. 4A and B), the structure of the HC is not clearly delineated from that of the MB zone; this is also manifest in the similar stiffness values of 24 ± 4 and 19 ± 1 kPa for the HC and MB zones, respectively. Proceeding toward the basal region, the collagen fibers gradually merge until they form a tightly packed structure at the basal region (Fig. 4C and D). On the covering net side of the TM (Fig. 4A and C), the HC zone has a structure consisting of transverse fibers. In the apical region (Fig. 4A), these fibers are arranged in a mesh-like pattern that greatly resembles the structure of the covering net. Toward the basal region, the collagen fibers become closer to each other until they form a uniform dense matrix that is clearly delineated from the neighboring MB zone (Fig. 4C). In agreement with the observed structural changes, the mechanical properties dramatically change as well. The stiffness of the dense fiber structure in the HC zone of the basal region (210 ± 15 kPa) is ≈ 10 times greater than their stiffness in the apical region (24 ± 4 kPa).

In agreement with Abnet and Freeman (27), our results show that the orientation of the covering net makes an insignificant

contribution to the measured mechanical properties of the TM (see Fig. 8 and *Supporting Text* which are published as supporting information on the PNAS web site). The negligible role of covering net orientation is probably due to its thickness (≈ 50 nm). Bueckle's indentation depth limit (28) states that, when the indentation depth is $>10\%$ of the sample thickness, the mechanical properties of the supported material begin to impact the measurement. The lowest indentation depth applied in our measurements (≈ 50 nm) is almost an order of magnitude larger than the Bueckle's limit for the covering net (≈ 5 nm). Our nanoindentation, and probably even more so, our microindentation measurements are likely to represent the mechanical properties of the TM's bulk material with a negligible contribution from the covering net. Unfortunately, it is not possible to gain information on the structure of the TM bulk by using SEM, because it can only image the surface of the TM. However, based on the results presented in this work, which indicate that the Young's modulus of the TM is identical on both sides, we suggest that the bulk structure on both sides of the TM is similar. Indeed, the structure of the TM beneath the covering net (Fig. 4C *Inset*) is similar to the structure seen from the opposite side of the TM (Fig. 4D).

Analysis of our results shows that the thickness of the TM, together with the arrangement of its fibers, affects its mechanical properties. A comparison between zones in the radial direction shows that the thickest region, the MB zone, is always the softest zone. By contrast, the thinnest region, the limbal zone, was found to be the stiffest region throughout the entire length of the TM except for the basal region. An important concern that should be addressed is associated with the possible contribution of the supporting stiff glass slide to the measured stiffness. This contribution, if it exists, would be larger in measurements carried out on thin regions of the TM than for those carried out on thicker regions, and would thus produce a false correlation between thickness and stiffness. To rule out this possibility, we estimated the thickness of the TM using fluorescence microscopy by placing fluorescently labeled beads between the glass-slide and the TM as well as on its surface. We found that even for the thinnest segment of the TM, the limbal zone at the basal end, the thickness was ≈ 10 μm . The largest indentation depths applied in this work (≈ 350 nm) are well below the limit defined by Bueckle's law for such a sample (≈ 1 μm). Therefore, we can rule out the possible contribution of the supporting glass to our measurements, and conclude that the observed correlation between thickness and stiffness reflects intrinsic properties of the TM. In further support of this finding, a similar correlation between thickness and stiffness was reported by Abnet and Freeman (27). They found that in mouse TM samples isolated from the apical region, thicker samples were softer than thinner ones. Zwislocki *et al.* (29) showed that the TM is less hydrated toward the limbal zone. Therefore, it is possible that the correlation between TM thickness and stiffness results from differences in the hydration levels of different TM segments. Interestingly, at the basal end of the TM, the HC zone is thicker than the limbal zone, yet it is significantly stiffer. This result suggests that in this region, the contribution of the collagen fiber arrangement to TM stiffness is greater than the softening contribution of thickness.

Conclusions and Implications

Previous mechanical property studies of other key structures located in the organ of Corti found differences along the cochlear length. For example, basilar membrane stiffness varies by a factor of 100 along the length of the cochlea, with lower stiffness values being measured toward the apical region (30). The stiffness values of OHC stereocilia gradually increase by two to three orders of magnitude from the apical to the basal region

of the cochlea (31, 32). The results presented in this work show a gradual increase in the stiffness of the TM in the HC zone, along the length of the cochlea. The HC zone of the TM is probably the most relevant region for understanding the mechanical role of the TM, because it is the zone where OHC stereocilia are physically embedded into the TM. The TM is soft in the low-frequency response region of the cochlea and stiffer in the high-frequency response region. The resonance frequency of a stiff material is higher than that of a soft one, thus it can respond at a higher frequency. Our findings suggest that the TM has selectivity in its frequency response along the cochlear partition, and that it is mechanically coupled with the stereocilia hair bundles. Such a mechanical coupling may prevent either damping or over-stimulation of the hair bundle motions. A similar active tunable TM was suggested by Brown *et al.* (33) over a decade ago.

An order of magnitude difference in stiffness values between the basal and apical regions of the TM is unlikely to sufficiently promote successful mechanical coupling throughout the entire functional audio frequency range (≈ 1 –90 kHz). However, the TM has been shown to behave as a viscoelastic material (21, 27), where its stiffness depends on the rate of stress or rate of strain. We predict that the mechanical differences observed in our pseudostatic measurements will be enhanced in dynamic-mechanical measurements conducted under physiologically relevant conditions, i.e., in the functional auditory frequency range at nanometer amplitudes. These measurements, which use a time-resolved AFM technique (34), are the focus of our current efforts.

Materials and Methods

Sample Preparation. TM samples were isolated from a total of 25 adult mice at ≈ 2 months of age. The cochlea was dissected and removed from the mouse and the TM was isolated by using a previously reported technique (27). During attachment of the TM to the Cell-Tak-coated glass slide, there was no control over the polarity of the TM, i.e., whether the covering net side of the TM faced up or down. Orientation of the sample was determined by transmission light microscopy. Samples that appeared to be folded or damaged in any way were discarded.

Isolated TM samples were classified according to three longitudinal regions (apical, mid-turn, and basal) based on their corresponding position along the cochlea. TM classification was further supported by analysis of sample dimensions. Narrow and thin samples were considered to be associated with the basal region of the cochlea, whereas wider and thicker samples were considered to be taken from the apical end. Samples that could not easily be assigned to either end were considered to be associated with the mid-turn region. In addition to the longitudinal association, each TM sample was subdivided into three radial zones: (i) HC, which represents the location of the region with imprints of OHC stereocilium, (ii) main body (MB), which represents the main body of the TM, which is located approximately above the IHCs, and (iii) limbal, which represents the zone at which the TM attaches to the spiral limbus. Radial zone assignments were carried out by inspecting the sample using transmission light microscopy (Fig. 1A).

AFM Indentation Experiments. The mechanical properties of the TM were measured by AFM operated in the force–distance mode. All AFM experiments were carried out by using a Bioscope with a Nanoscope IV controller (Veeco, Santa Barbara, CA) that is mounted on an inverted optical microscope (Axiovert 200M, Carl Zeiss, Heidelberg, Germany). Indentation experiments were carried out with silicon nitride triangular cantilevers (DNP) having a nominal spring constant of 0.06 N/m. Cantilever spring constants were determined experimentally by measuring their thermal fluctuations (35).

For nanometer-scale indentations, square-based pyramidal tips with a nominal radius of ≈ 20 nm were used, whereas borosilicate spherical probes with a radius of ≈ 1 μm (Bioforce, Ames, IA) were used for micrometer scaled indentation measurements. For data analysis, results were grouped according to the radial and longitudinal position of the corresponding TM sample (see Fig. 1). For each indentation measurement, ≈ 150 force–distance curves were performed at a scan rate of 2 Hz. To maintain a constant maximal loading force, the deflection of the cantilever was limited by a trigger. For nanometer-sized probes, the maximal deflection was 0.5 V (corresponding to a loading force of 3 nN), whereas for micrometer-sized probe, the maximal deflection was 5 V (corresponding to a 30 nN loading force).

Data analysis for calculating the TM point stiffness was carried out according to a method commonly used in our laboratory (36). For Young's modulus estimation, indentation experiments carried out by using nanometer-scaled indenter were analyzed according to a described model (37). For measurements con-

ducted with a micrometer-size spherical indenter a modified Hertz model was used (37). Finite-element simulations were carried out by using the MSC.MARC software.

Electron Microscopy. Isolated samples of the cochlea were permeabilized by incubation with a solution of 2% glutaraldehyde in 0.1 M sodium cacodylate buffer (pH 7.4) for 15 min. Exposed TM pieces were viewed and photographed by using an environmental scanning electron microscope (Phillips XL-30).

Additional details on data analysis and EM imaging are provided in *Supporting Text*.

We thank Yehudit Hermesh for technical assistance in the surgical procedures performed on the animals and Orna Yeger and Stella Izhakov for their help with sample preparation for SEM analysis. This work was supported in part by Israel Science Foundation Grant 26/05, a grant from the Jean-Jacques Brunschwig Fund for the Molecular Genetics of Cancer, and the Kimmelman Center for Macromolecular Assemblies. I.R. is the incumbent of the Robert Edwards and Roselyn Rich Manson Career Development Chair.

1. Thalmann I, Machiki K, Calabro A, Hascall VC, Thalmann R (1993) *Arch Biochem Biophys* 307:391–396.
2. Brownell WE, Bader CR, Bertrand D, de Ribaupierre Y (1985) *Science* 227:194–196.
3. Hudspeth AJ (2005) *C R Biol* 328:155–162.
4. Spoendlin H (1985) *Am J Otolaryngol* 6:453–467.
5. Legan PK, Rau A, Keen JN, Richardson GP (1997) *J Biol Chem* 272:8791–8801.
6. McGuirt WT, Prasad SD, Griffith AJ, Kunst HP, Green GE, Shpargel KB, Runge C, Huybrechts C, Mueller RF, Lynch E, et al. (1999) *Nat Genet* 23:413–419.
7. Pfister M, Thiele H, Van Camp G, Fransen E, Apaydin F, Aydin O, Leisten-schneider P, Devoto M, Zenner HP, Blin N, et al. (2004) *Cell Physiol Biochem* 14:369–376.
8. Jacobson J, Jacobson C, Gibson W (1990) *J Am Acad Audiol* 1:37–40.
9. Davis H (1965) *Cold Spring Harb Symp Quant Biol* 30:181–190.
10. Billone M, Raynor S (1973) *J Acoust Soc Am* 54:1143–1156.
11. Neely ST, Kim DO (1983) *Hear Res* 9:123–130.
12. Geisler CD (1986) *Hear Res* 24:125–131.
13. Kolston PJ (1988) *J Acoust Soc Am* 83:1481–1487.
14. Zwislocki JJ, Kletsky EJ (1979) *Science* 204:639–641.
15. Allen JB (1980) *J Acoust Soc Am* 68:1660–1670.
16. Zwislocki JJ (1980) *J Acoust Soc Am* 67:1679–1685.
17. Gummer AW, Hemmert W, Zenner HP (1996) *Proc Natl Acad Sci USA* 93:8727–8732.
18. Mammano F, Nobili R (1993) *J Acoust Soc Am* 93:3320–3332.
19. Bekesy GV (1960) *Experiments in Hearing* (McGraw-Hill, New York).
20. Zwislocki JJ, Cefaratti LK (1989) *Hear Res* 42:211–227.
21. Freeman DM, Abnet CC, Hemmert W, Tsai BS, Weiss TF (2003) *Hear Res* 180:1–10.
22. Shoelson B, Dimitriadis EK, Cai H, Kachar B, Chadwick RS (2004) *Biophys J* 87:2768–2777.
23. Stolz M, Raiteri R, Daniels AU, VanLandingham MR, Baschong W, Aebi U (2004) *Biophys J* 86:3269–3283.
24. Hasko JA, Richardson GP (1988) *Hear Res* 35:21–38.
25. Thalmann I, Thallinger G, Crouch EC, Comegys TH, Barrett N, Thalmann R (1987) *Laryngoscope* 97:357–3567.
26. Slepecky NB, Savage JE, Cefaratti LK, Yoo TJ (1992) *Cell Tissue Res* 267:413–418.
27. Abnet CC, Freeman DM (2000) *Hear Res* 144:29–46.
28. Bueckle H (1973) *The Science of Hardness Testing and its Research Applications* (Am Soc for Metals, Materials Park, OH).
29. Zwislocki JJ, Chamberlain SC, Slepecky NB (1988) *Hear Res* 33:207–222.
30. Naidu RC, Mountain DC (1998) *Hear Res* 124:124–131.
31. Geleoc GS, Lennan GW, Richardson GP, Kros CJ (1997) *Proc Biol Sci* 264:611–621.
32. Russell IJ, Kossl M, Richardson GP (1992) *Proc Biol Sci* 250:217–227.
33. Brown AM, Gaskill SA, Williams DM (1992) *Proc Biol Sci* 250:29–34.
34. Anwar M, Rouso I (2005) *Appl Phys Lett* 86:014101.
35. Hutter J, Bechheoffer J (1993) *Rev Sci Instr* 64:1868–1873.
36. Kol N, Gladnikoff M, Barlam D, Shneck RZ, Rein A, Rouso I (2006) *Biophys J* 91:767–774.
37. Vinckier A, Semenza G (1998) *FEBS Lett* 430:12–16.